

Very fast light-induced degradation of *a*-Si:H/*c*-Si(100) interfaces

Stefaan De Wolf,* Bénédicte Demaurex, Antoine Descoedres, and Christophe Ballif

École Polytechnique Fédérale de Lausanne (EPFL), Institute of Microengineering (IMT), Photovoltaics and Thin Film Electronics Laboratory, Rue A.-L. Breguet 2, CH-2000 Neuchâtel, Switzerland

(Received 14 January 2011; revised manuscript received 21 April 2011; published 7 June 2011)

Light-induced degradation (LID) of crystalline silicon (*c*-Si) surfaces passivated with hydrogenated amorphous silicon (*a*-Si:H) is investigated. The initial passivation decays on polished *c*-Si(100) surfaces on a time scale much faster than usually associated with bulk *a*-Si:H LID. This phenomenon is absent for the *a*-Si:H/*c*-Si(111) interface. We attribute these differences to the allowed reconstructions on the respective surfaces. This may point to a link between the presence of so-called “fast” states and (internal) surface reconstruction in bulk *a*-Si:H.

DOI: [10.1103/PhysRevB.83.233301](https://doi.org/10.1103/PhysRevB.83.233301)

PACS number(s): 73.20.Hb, 42.50.Ct, 71.55.Jv, 72.20.Jv

Hydrogenated amorphous silicon (*a*-Si:H) is a semiconductor with important applications in a host of large-area electronic devices, including solar cells.¹ In recent years, the interface between *a*-Si:H and crystalline silicon (*c*-Si) has received increased attention because *a*-Si:H films passivate *c*-Si surfaces remarkably well. This allows for the fabrication of high-efficiency *a*-Si:H/*c*-Si heterojunction solar cells at low temperature (<200 °C), with efficiencies of up to 23% reported to date.² For thin-film microcrystalline silicon (μ *c*-Si:H) solar cells, the *a*-Si:H/*c*-Si interface is of equal importance as device-grade μ *c*-Si:H consists of nanometer-sized *c*-Si grains embedded in an *a*-Si:H matrix.¹ For atomically sharp interfaces,³ passivation by intrinsic *a*-Si:H films stems from hydrogenation of *c*-Si surface states,⁴ and near-surface *a*-Si:H bulk defects.⁵ Characteristically, *a*-Si:H bulk material suffers from the so-called Staebler-Wronski effect (SWE).⁶ This is manifested by (self-limiting) light-induced generation of electronically active defects,⁷ most likely as Si dangling bonds.^{8,9} The increase in Si dangling bond density is detrimental for device performance. Even though the microscopic origin of this defect is still under debate,¹⁰ it is often linked to how hydrogen is bonded to silicon in the *a*-Si:H films.^{11,12}

In this article we investigate the influence of light soaking on *a*-Si:H films deposited on *c*-Si surfaces of two different crystal orientations: *c*-Si(100) and *c*-Si(111). The use of high-grade *c*-Si surfaces combined with carrier-lifetime measurements in the wafer gives us a uniquely sensitive tool to probe the influence of different interfacial silicon-hydrogen bonding configurations on the electronic properties during light exposure. We confirm that light-induced degradation (LID) occurs in *a*-Si:H/*c*-Si structures by dangling-bond creation.¹³ At very short exposure times we observe strong crystal-orientation dependence, however. This may point to a link between the presence of so-called “fast” states in *a*-Si:H and (internal) surface reconstruction in the films.

For the experiments, ~280- μ m-thick ~4.0- Ω cm phosphorus-doped mirror-polished float-zone *c*-Si(100) and *c*-Si(111) wafers from Topsil were used. Surface cleaning consisted of native oxide stripping in a dilute HF solution (4%) for 45 s, after which the samples were immediately transferred to the deposition systems. Intrinsic *a*-Si:H films (thickness of ~50 nm) were codeposited on the *c*-Si(100) and *c*-Si(111) substrates. For this, a narrow-gap (13 mm), parallel-plate plasma-enhanced chemical vapor deposition reactor powered at very-high frequency (40.68 MHz) was used. The deposition

temperature T_{depo} was set at 200 °C; other processing details are described elsewhere.¹⁴ On glass, such films yield an optical band gap of 1.68 eV, determined from spectroscopic ellipsometry. We also tested *c*-Si wafers passivated with aluminum-oxide (Al₂O₃) films.¹⁵⁻¹⁷ Such films (thickness of ~30 nm) were prepared by alternating trimethylaluminum [Al(CH₃)₃] exposure and a remote O₂ plasma using a plasma-assisted atomic layer deposition reactor; typical deposition and activation-annealing conditions are described elsewhere.¹⁷ These samples served as a benchmark against which the *a*-Si:H/*c*-Si structures were compared. In all cases, films were deposited on both sides of each wafer to evaluate the surface passivation quality. Following this, the samples were subjected to low-temperature hot-plate annealing (220 °C in air), and subsequent light-soaking for prolonged times. The latter was done at ~50 °C under a standard 1-sun (100 mW cm⁻²) air mass 1.5-global (AM 1.5 G) spectrum. The effective carrier lifetime of the samples, τ_{eff} , is a direct indicator of the passivation quality and was measured at room temperature with a Sinton Consulting WCT-100 photo conductance system operated in transient mode.¹⁸ The annealing or light-soaking treatments were briefly interrupted for these measurements. Finally, thermal desorption spectroscopy (TDS) was used to characterize the surfaces immediately after HF termination; details are described elsewhere.¹⁹

Figure 1(a) shows how τ_{eff} changes under prolonged annealing at 220 °C for the respective structures. The initial τ_{eff} values are very similar for the *a*-Si:H/*c*-Si(100) and *a*-Si:H/*c*-Si(111) samples. These data sets can be fitted to stretched exponentials, pointing to local rearrangement of hydrogen at the interface.⁴ Notably, values for τ_{eff} of 8–10 ms are obtained which are among the highest reported for such structures. The same panel also gives data for Al₂O₃/*c*-Si(100) structures. Here, annealing leads to a slight decrease in passivation. This behavior contrasts with the effect of the initial postdeposition anneal needed to activate the surface-passivation properties of Al₂O₃ films.^{16,17} The observed decrease may be linked to *in situ* hydrogenation of Al₂O₃/*c*-Si interface charge carrier traps, resulting in a lower fixed-charge density,²⁰ and consequently less repulsion of electrons from the interface.

Figure 1(b) gives τ_{eff} data for the same samples as in panel (a), but now during 1-sun light soaking up to 500 h. After as little as 1 min, τ_{eff} of the *a*-Si:H/*c*-Si(100) structure unexpectedly drops by close to 40% (see arrow). Such a drop is absent for both the *a*-Si:H/*c*-Si(111) and the Al₂O₃/*c*-Si(100) structures. Prolonged light soaking of the *a*-Si:H/*c*-Si(100)

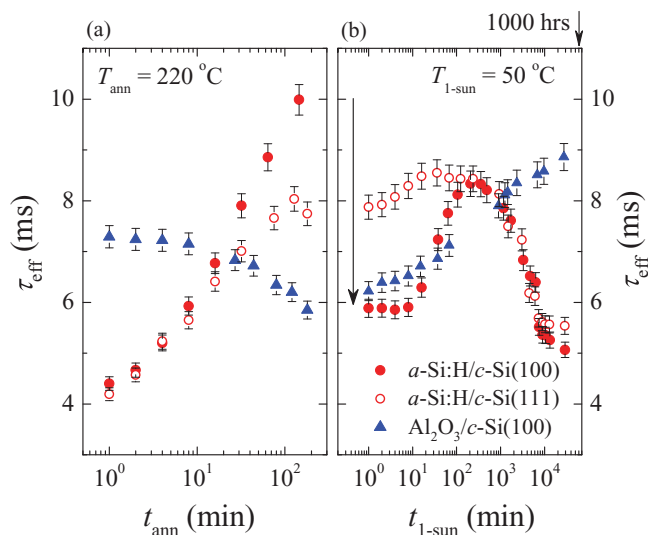


FIG. 1. (Color online) Changes in τ_{eff} for the different test structures. (a) Influence of low-temperature annealing in air. (b) Influence of prolonged 1-sun exposure. Measurements at $\Delta n = 1.0 \times 10^{15} \text{ cm}^{-3}$.

structures leads then to an improvement. After ~ 6 h, steady decay sets in, however. A smaller initial improvement occurs for the $a\text{-Si:H/c-Si(111)}$ structure, and again after ~ 6 h decay sets in. Notably, the long-term degradation of the two surfaces is almost indistinguishable. Also, for both structures, reannealing at $220 \text{ }^\circ\text{C}$ fully reinitializes the samples (not shown), indicating metastability.

The $\text{Al}_2\text{O}_3/\text{c-Si(100)}$ structure shows quite a different behavior. Here, a significant monotonic light-induced improvement in τ_{eff} is observed. The improvement in passivation of this structure is likely caused by a light-induced increase of negative fixed charge Q_f at its interface. Briefly, UV exposure may lead to an increase of Q_f in Al_2O_3 films,¹⁵ without much influence on the interface-state density D_{it} . This effect is linked to internal photoemission (IPE) of electrons from the $c\text{-Si}$ valence-band maximum into the Al_2O_3 conduction-band minimum. It can also occur under intense lower-energy illumination, where the electron pumping is now achieved by multiphoton IPE.²¹ In any case, the improvement for the $\text{Al}_2\text{O}_3/\text{c-Si(100)}$ structure strongly suggests that the bulk of the $n\text{-type c-Si}$ wafers used does not degrade under light soaking. Consequently, the observed $a\text{-Si:H/c-Si}$ light-soaking phenomena can almost certainly be attributed to the $a\text{-Si:H}$ films and the interface they share with the specific $c\text{-Si}$ surfaces.

To discuss the long-term light-soaking behavior, Fig. 2(b) shows dangling-bond densities, N_{DB} , for the $a\text{-Si:H/c-Si(100)}$ structure. For this, the τ_{eff} data given in Fig. 1 were plotted over their full carrier-injection range and fitted to an appropriate surface-recombination model [Fig. 2(a)].²² The two major model parameters are the surface dangling-bond density N_{DB}^S and the fixed-charge density Q_f . The latter parameter comprises all contributions to the surface potential, including interface trapped charge, fixed charges in the film, and band offsets at the $a\text{-Si:H/c-Si}$ interface. Dangling bonds are electronically characterized by their electron and hole capture cross sections, respectively, in the neutral state, σ_n^0 and σ_p^0 , and the charged state, σ_n^+ and σ_p^- . The following ratios, similar to $a\text{-Si:H}$

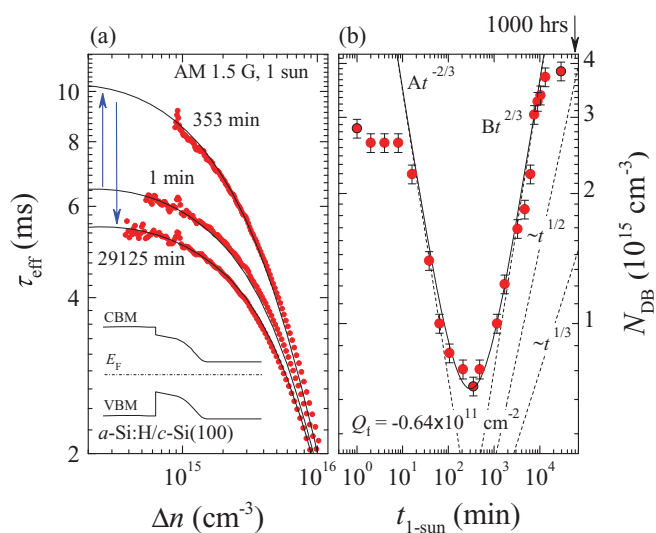


FIG. 2. (Color online) (a) Changes in τ_{eff} (Δn) for an $a\text{-Si:H/c-Si(100)}$ structure during prolonged 1-sun exposure. Symbols are measured data, solid lines are fits using recombination-model calculations. For clarity, only a few selected examples are shown. The inset shows the band diagram of the interface in (dark) thermal equilibrium, simulated with AFORS-HET. (b) Dangling-bond density N_{DB} of the same structure, extracted from the fitting shown in (a). The lines are fits to power laws. Fitting parameters are $A = 0.27 \times 10^{15} \text{ cm}^{-3} \text{ s}^{-1}$ and $B = 0.13 \times 10^{12} \text{ cm}^{-3} \text{ s}^{-1}$. For reference, we also show $\sim t^{1/3}$ and $\sim t^{1/2}$ power laws.

bulk, were found for the interface dangling-bond capture cross sections²²: $\sigma_p^0/\sigma_n^0 = 20$ and $\sigma_n^+/\sigma_n^0 = \sigma_p^-/\sigma_p^0 = 500$. Following Schulze *et al.*⁵ we assume $\sigma_p^0 = 10^{-18} \text{ cm}^2$. For all fits and for both surface orientations only N_{DB}^S required adjustment, whereas Q_f could be kept constant at $-0.64 \times 10^{11} \text{ cm}^{-2}$. This shows that the surface-state density changes upon light soaking and not the surface band bending, within fitting error. As such, it suggests that the observed light-induced changes are driven by changes in dangling-bond density. Finally, we converted N_{DB}^S to an equivalent *ad hoc* “bulk” density, $N_{\text{DB}} = (N_{\text{DB}}^S)^{3/2}$.

Following the fast LID, N_{DB} decreases under 1-sun illumination for several hours for the $a\text{-Si:H/c-Si(100)}$ structure. After about 6 h of light exposure, N_{DB} starts to increase monotonically, however. Both phenomena (i.e., the sequential decrease and increase in N_{DB}) can be nearly fit to, respectively, $\sim t^{-2/3}$ and $\sim t^{2/3}$ power laws, as seen in Fig. 2(b). The data show saturation, likely pointing to the self-limiting nature of the SWE.⁷ A better estimate for N_{DB} may be N_{DB}^S divided by the (unfortunately unknown) probing depth of the wave function into the $a\text{-Si:H}$ film, yielding $\sim t^{\pm 4/9}$ laws. For both N_{DB} estimations, the long-term degradation is faster than the familiar $\sim t^{1/3}$ law characteristic for bulk $a\text{-Si:H}$ material.⁷ In films on glass, intense illumination (resulting in higher excess-carrier densities) is known to yield an increase in N_{DB} faster than the $\sim t^{1/3}$ law.²³ Considering this, we attribute the observed faster decay under 1-sun illumination to possible differences in carrier-injection exposure of $a\text{-Si:H}$ bulk states compared to states close to the $a\text{-Si:H/c-Si}$ interface. For films on high-grade $c\text{-Si}$ wafers, excess carriers recombining through states in the vicinity of this interface may have been generated either in the film or in the wafer. As such,

under identical illumination, near-surface states are likely exposed to higher excess-carrier densities than their bulk a -Si:H counterparts, explaining the faster decay.

The observed defect reduction and subsequent creation as shown in Fig. 2(b) points to a kinetic process for the total defect density that cannot be described by a single rate equation. Rather, more than one type of defect with different kinetic characteristics may be present. Such conclusion was drawn earlier for bulk a -Si:H material based on a two-step high-low intensity light-soaking experiment, identifying so-called “fast” and “slow” defects.²⁴ Here, considering the identical long-term degradation behavior for both surface orientations [see tails in Fig. 1(b)], the slow defect could be linked to the (identical) near-surface a -Si:H bulk of these thin layers, whereas the fast defect may rather be linked to their specific interface. Alternatively, the kinetics could be interpreted as due to the combined effect of defect creation and (de-)trapping of interface charge.

We now turn to the discussion of the fast initial decay observed in the a -Si:H/ c -Si(100) structure. Figure 3(a) gives more detailed information on this phenomenon by comparing

the normalized changes in τ_{eff} during flash-light exposure at room temperature for the same codeposited a -Si:H/ c -Si(100) and a -Si:H/ c -Si(111) samples. Each flash is <1 ms long and is the same flash as used during lifetime measurements. Prior to the experiment, the samples were reinitialized by annealing at 220 °C. The earlier observed differences between these two surfaces are confirmed in this graph. For the a -Si:H/ c -Si(111) structure the initial passivation is relative stable, whereas for the a -Si:H/ c -Si(100) case a smooth single-exponential decay occurs. Figure 3(b) shows that following exposure the passivation slowly (and partially) recovers at room temperature in dark. Full recovery is achieved by brief annealing (2 min at 220 °C; see arrow). Figure 3(c) shows calculated values for N_{DB} for one cycle, following the earlier outlined conversion procedure. Again, the value of Q_f could be kept constant for all fits. The observed metastability must be linked to the specific a -Si:H/ c -Si interface and not to the c -Si bulk because identical c -Si(100) wafers were used for the field-effect passivated Al_2O_3 / c -Si(100) structures which did not show such behavior [Fig. 1(b)]. Next, since the a -Si:H films were codeposited on both surfaces, this phenomenon is likely caused by surface-orientation specific defect states.

Carrier trapping can influence transient τ_{eff} data for many surface passivation layers, including a -Si:H, as argued by Seiffe *et al.*²⁵ For these films, higher time-integrated carrier injection (e.g., by more intense flashes) prior to τ_{eff} acquisition yields increased excess hole densities at the interface [see also simulated band diagram of our a -Si:H(i)/ c -Si(n) interface in the inset of Fig. 2(a)]. Such holes may be trapped at interface states, yielding *increased* (field-effect mediated) passivation.²⁵ Our τ_{eff} data contrast with this. Firstly, we observe *decreased* passivation with increasing time-integrated light exposure. Secondly, our results show strong surface-orientation dependence. Finally, the occurrence of slow and incomplete room-temperature recovery suggests a rather more persistent phenomenon that is not purely driven by charge (de-)trapping.

Alternatively, the fast metastability may be caused by surface-orientation specific defect formation and annihilation. Shinohara *et al.*, provided evidence that hydrogenated (di-)vacancies are created beneath Si(100) surfaces when exposed to atomic hydrogen.²⁶ No such defects were observed beneath Si(111) surfaces.²⁶ At present, it cannot be excluded that similar defects form during a -Si:H deposition, potentially acting as a degradation culprit.

The interaction of hydrogen with the actual c -Si surface is perhaps better understood. For example, by immersion of the Si(111) surface in HF-based solutions, extremely well-passivated surfaces were demonstrated with surface-recombination velocities down to 0.25 cm s^{-1} (Ref. 27). This was linked to ideal hydrogen termination of this surface (in buffered solutions) yielding the Si(111)-(1 × 1):H structure, where each silicon surface atom has a single, hydrogenated, dangling bond.²⁸ Figure 3(d) gives TDS data of our c -Si(111) surfaces following HF etching, and prior to film deposition. The dominant higher temperature peak β_1 points to monohydride termination. We attribute the much smaller β_2 peak to higher hydrides present at the cleaved sample edges or possible steps. The interaction of hydrogen with the c -Si(100) surface is quite different: For this surface, each (unreconstructed) surface atom features two dangling bonds,

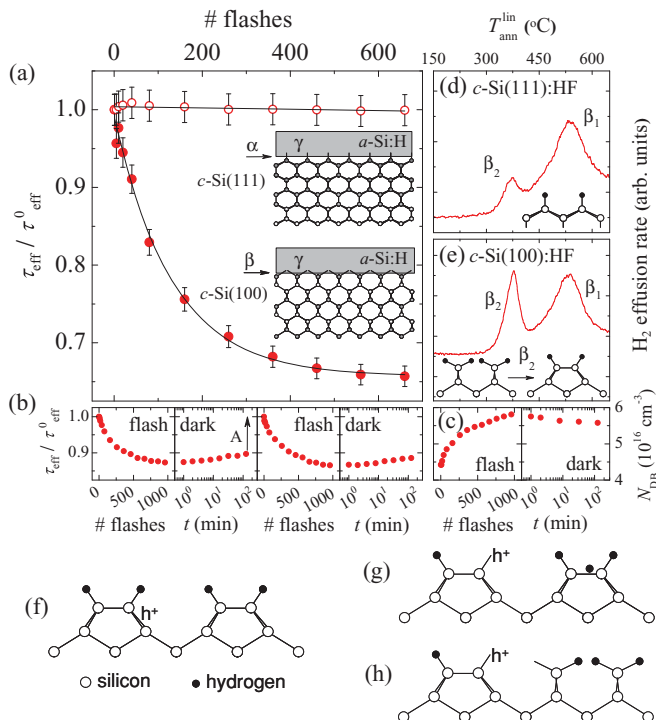


FIG. 3. (Color online) (a) Normalized τ_{eff} values for a -Si:H/ c -Si(100) (closed symbols) and a -Si:H/ c -Si(111) (open symbols) structures during flash-light exposure. Each flash is ~ 1 ms long. Measurements are evaluated at $\Delta n = 1.0 \times 10^{15} \text{ cm}^{-3}$. The lines are linear and single-exponential fits. The insets represent the two different test structures featuring identical capping films, γ , but different interfaces, α and β . (b) Normalized τ_{eff} values for a different a -Si:H/ c -Si(100) structure during repeated cycles of flash-light exposure, dark relaxation at room temperature and annealing (220 °C for 2 min, see arrow). (c) Calculated N_{DB} values corresponding to data in (b). (d) and (e) H_2 -effusion rate data for HF-terminated c -Si(111) and c -Si(100) surfaces, respectively, prior to film deposition. Heating rate was 20 K min^{-1} . Insets show the different surface structures schematically. (f)–(h) Schematic representation of the SWE model by Carlson. See main text for explanation.

possibly hydrogenated.²⁹ Figure 3(e) gives TDS data of our *c*-Si(100) surfaces following HF etching. The low-temperature β_2 state is associated with higher hydrides where annealing may transform (adjacent) Si(100)-(1 × 1):2H structures to doubly occupied Si(100)-(2 × 1):H dimers by simultaneous rupture of two Si-H bonds, forming a H₂ molecule in the process [see also inset in Fig. 3(e)]. The β_1 state again is rather a signature for monohydride termination.³⁰

In bulk *a*-Si:H, mono and higher hydrides are present too, depending on the deposition conditions. Monohydrides are often associated with the divacancy defect, whereas higher hydrides are rather present at hydrogenated internal nanometer-sized voids or surfaces.³¹ The presence of the latter is usually undesirable from an electronic point of view. Dense films with low void density show superior light-soaking stability.¹² Other studies equally assigned a key role to *paired* hydrogen atoms in the understanding of the SWE.³²

Of particular significance to our work is the SWE model developed by Carlson.¹¹ Essentially, this model links the SWE to surface reconstruction of internal voids, inspired by reconstructions allowed for the Si(100) surface.²⁹ We briefly repeat here its most salient features:¹¹ Light-generated holes can be trapped near voids in the *a*-Si:H bulk. For simplicity, the void surface is assumed to be similar to the hydrogenated Si(100) surface [Fig. 3(f)]. Subsequent motion of these holes can induce the motion of atomic hydrogen on internal surfaces [Fig. 3(g)], which may rupture a Si(100)-(2 × 1):H dimer [Fig. 3(h)]. Further reconstructing may occur (not shown). Low-temperature annealing yields reconstruction back to the initial (lower-energy) dimer state.

Considering this model, we propose that the fast LID is linked to the specific Si(100) surface chemistry where light soaking results in dimer rupture and subsequent low-temperature annealing reconstructs the dimers. This leads respectively to deteriorated and improved passivation. The main difference between our experimental *a*-Si:H/*c*-Si(100) interfaces and the idealized model is the *a*-Si:H capping of

the “internal” surface [indicated respectively by γ and β in the inset of Fig 3(a)]. Reconciling this difference with the model suggests the presence of (nano-sized) hydrogen platelets at the interface. For as-deposited material, hydride modes at higher stretching frequencies are known to be more dominant close to the interface rather than several nanometers into the *a*-Si:H film.³³ The drastic initial improvement in passivation by annealing [Fig. 1(a)] also points to relatively disordered films at the interface,⁴ possibly accommodating such platelets. Our experimental *a*-Si:H/*c*-Si(111) structures can equally be regarded as an idealized “internal” surface capped by bulk *a*-Si:H material [indicated respectively by α and γ in the inset of Fig 3(a)]. No reconstruction is expected for hydrogenated Si(111) surfaces.³⁴ Consistently, no fast LID is observed either for this surface. Finally, we remark that (incomplete) room-temperature annealing of bulk *a*-Si:H material has been associated with the presence of earlier mentioned fast states.^{24,35} As such, it is tempting to conclude that fast states in *a*-Si:H material must be linked to structures similar to those specifically present at the *c*-Si(100) surface.

To summarize, 1-sun light soaking yields degradation in passivation of the *a*-Si:H/*c*-Si interface, contrasting with the improvement of passivation for its Al₂O₃/*c*-Si counterpart. The degradation follows a power law, even though it may take time to observe it. The detailed kinetics suggest the presence of more than one type of defect. Upon very short exposure times clear differences between *c*-Si(111) and *c*-Si(100) surfaces are observed, which we interpret as due to a fast defect possibly linked to *c*-Si(100) surface reconstruction.

We thank G. Dingemans, M. C. M. van de Sanden, and W. M. M. Kessels for the Al₂O₃ depositions; R. Bartlome, F.J. Haug, and J. Holovsky for useful discussions, and S. Olibet for providing the recombination-model source code. This work was supported by the European Community’s FP7 Programme under the 20Pl μ s Project (Grant Agreement No. 256695), and by Axp0 Naturstrom Fonds, Switzerland.

*stefaan.dewolf@epfl.ch

¹A. Shah, P. Torres *et al.*, *Science* **285**, 692 (1999).
²T. Mishima *et al.*, *Solar Energy Materials and Solar Cells* **95**, 18 (2011).
³S. De Wolf and M. Kondo, *Appl. Phys. Lett.* **90**, 042111 (2007).
⁴S. De Wolf *et al.*, *Appl. Phys. Lett.* **93**, 032101 (2008).
⁵T. F. Schulze *et al.*, *Appl. Phys. Lett.* **96**, 252102 (2010).
⁶D. L. Staebler and C. R. Wronski, *Appl. Phys. Lett.* **31**, 292 (1977).
⁷M. Stutzmann *et al.*, *Phys. Rev. B* **32**, 23 (1985).
⁸I. Hirabashi *et al.*, *Jpn. J. Appl. Phys.* **19**, L357 (1980).
⁹H. Dersch *et al.*, *Appl. Phys. Lett.* **38**, 456 (1981).
¹⁰H. Fritzsche, *Annu. Rev. Mater. Res.* **31**, 47 (2001).
¹¹D. E. Carlson, *Appl. Phys. A* **41**, 305 (1986).
¹²E. Bhattacharya and A. H. Madan, *Appl. Phys. Lett.* **52**, 1587 (1988).
¹³H. Plagwitz *et al.*, *J. Appl. Phys.* **103**, 094506 (2008).
¹⁴A. Descoedres *et al.*, *Appl. Phys. Lett.* **97**, 183505 (2010).
¹⁵R. Hezel and K. Jaeger, *J. Electrochem. Soc.* **136**, 518 (1989).
¹⁶G. Agostinelli *et al.*, *Solar Energy Materials and Solar Cells* **90**, 3438 (2006).

¹⁷B. Hoex *et al.*, *Appl. Phys. Lett.* **89**, 042112 (2006).
¹⁸R. A. Sinton and A. Cuevas, *Appl. Phys. Lett.* **69**, 2510 (1996).
¹⁹S. De Wolf and M. Kondo, *J. Appl. Phys.* **105**, 103707 (2009).
²⁰S. Zafar *et al.*, *Appl. Phys. Lett.* **81**, 2608 (2002).
²¹J. J. H. Gielis *et al.*, *J. Appl. Phys.* **104**, 073701 (2008).
²²S. Olibet *et al.*, *Phys. Rev. B* **76**, 035326 (2007).
²³M. Stutzmann *et al.*, *Phys. Rev. Lett.* **67**, 2347 (1991).
²⁴L. Yang and L. Chen, *Appl. Phys. Lett.* **63**, 400 (1993).
²⁵J. Seiffe *et al.*, *J. Appl. Phys.* **109**, 064505 (2011).
²⁶M. Shinohara *et al.*, *J. Vac. Sci. Technol. A* **21**, 25 (2003).
²⁷E. Yablonovitch *et al.*, *Phys. Rev. Lett.* **57**, 249 (1986).
²⁸G. S. Higashi *et al.*, *Appl. Phys. Lett.* **56**, 656 (1990).
²⁹T. Sakurai and H. D. Hagstrum, *Phys. Rev. B* **14**, 1593 (1976).
³⁰M. P. D’Evelyn *et al.*, *J. Chem. Phys.* **96**, 852 (1992).
³¹A. H. M. Smets and M. C. M. van de Sanden, *Phys. Rev. B* **76**, 073202 (2007).
³²T. Su *et al.*, *Phys. Rev. Lett.* **89**, 015502 (2002).
³³H. Fujiwara and M. Kondo, *Appl. Phys. Lett.* **86**, 032112 (2005).
³⁴K. Hricovini *et al.*, *Phys. Rev. Lett.* **70**, 1992 (1993).
³⁵J. M. Pearce *et al.*, *Mater. Res. Soc. Symp. Proc.* **808**, A2.5.1 (2004).